RadioGraphics

Imaging of the Diaphragm: Anatomy and Function[1]

Laura K. Nason, MD • Christopher M. Walker, MD • Michael F. McNeeley, MD • Wanaporn Burivong, MD • Corinne L. Fligner, MD • J. David Godwin, MD

ONLINE-ONLY CME

This journal-based CME activity has been approved for ***AMA PRA Category 1 Credit™****. See www.rsna.org/education/rg_cme.html*

LEARNING OBJECTIVES

After completing this journal-based CME activity, participants will be able to:

- Discuss the embryology and anatomy of the diaphragm and the origin of diaphragmatic hernias.
- Describe normal diaphragmatic function and the causes of diaphragmatic dysfunction.
- Explain the fluoroscopic sniff test and list imaging findings suggestive of diaphragmatic dysfunction.

TEACHING POINTS

See last page

The diaphragm is the primary muscle of ventilation. Dysfunction of the diaphragm is an underappreciated cause of respiratory difficulties and may be due to a wide variety of entities, including surgery, trauma, tumor, and infection. Diaphragmatic disease usually manifests as elevation at chest radiography. Functional imaging with fluoroscopy (or ultrasonography or magnetic resonance imaging) is a simple and effective method of diagnosing diaphragmatic dysfunction, which can be classified as paralysis, weakness, or eventration. Diaphragmatic paralysis is indicated by absence of orthograde excursion on quiet and deep breathing, with paradoxical motion on sniffing. Diaphragmatic weakness is indicated by reduced or delayed orthograde excursion on deep breathing, with or without paradoxical motion on sniffing. Eventration is congenital thinning of a segment of diaphragmatic muscle and manifests as focal weakness. Treatment of diaphragmatic paralysis depends on the cause of the dysfunction and the severity of the symptoms. Treatment options include plication and phrenic nerve stimulation. Supplemental material available at *http://radiographics.rsna.org/lookup/suppl/doi:10.1148/rg.322115127/-/DC1*.

Introduction

The diaphragm is both the physical barrier that separates the thorax from the abdomen and the primary muscle of ventilation. Its dysfunction is a frequent contributor to dyspnea. Despite its importance, the diaphragm is often underappreciated and incompletely evaluated by clinicians and radiologists.

In this article, we review the embryology, anatomy, and function of the diaphragm and outline the classification, causes, and manifestations of diaphragmatic dysfunction, including paralysis, weakness, and eventration. Functional imaging of the diaphragm is discussed with a focus on the fluoroscopic sniff test, which is underused and easy to perform. Our technique and method of interpretation are reviewed, and key findings are illustrated with animations and cine clips. Ultrasonography (US) and magnetic resonance (MR) imaging of the diaphragm are also discussed. Finally,

Abbreviations: IVC = inferior vena cava, 3D = three-dimensional

RadioGraphics 2012; 32:E51–E70 • **Published online** 10.1148/rg.322115127 • **Content Code:** CH

[1]From the Departments of Radiology (L.K.N., C.M.W., M.F.M., J.D.G.) and Pathology (C.L.F.), University of Washington Medical Center, 1959 NE Pacific St, Box 357115, Seattle, WA 98195; and Department of Radiology, Srinakharinwirot University, Ongkarak, Thailand (W.B.). Recipient of a Certificate of Merit award for an education exhibit at the 2010 RSNA Annual Meeting. Received June 1, 2011; revision requested July 1 and received August 11; accepted August 12. For this journal-based CME activity, the authors C.M.W., C.L.F., and J.D.G. have disclosed various financial relationships (see p E69); all other authors, the editor, and reviewers have no relevant relationships to disclose. **Address correspondence to** J.D.G. (e-mail: *godwin@uw.edu*).

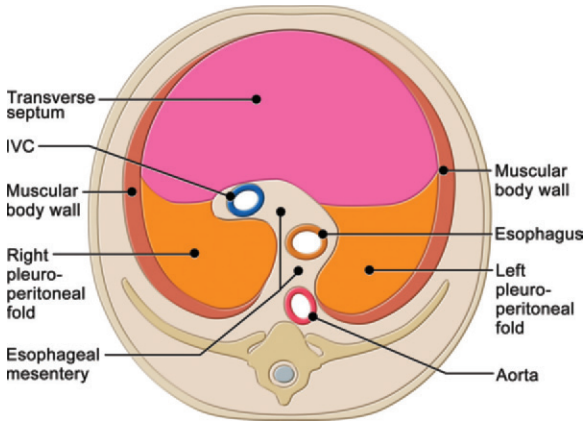

Figure 1. Development of the diaphragm. Schematic (view from below) shows that the diaphragm develops by fusion of four structures: the paired pleuroperitoneal folds, esophageal mesentery, transverse septum, and muscular body wall. *IVC* = inferior vena cava.

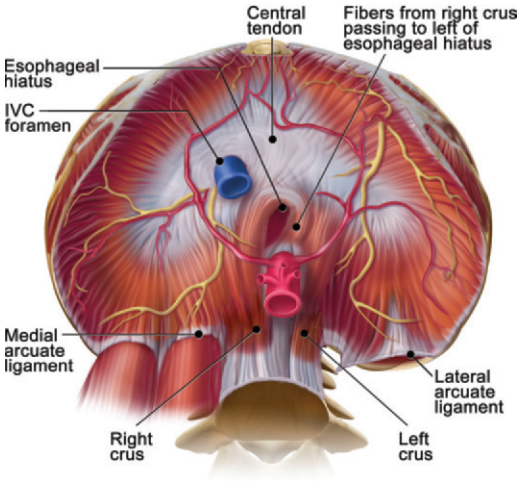

Figure 2. Drawing (view from below) shows the large central tendon, which is formed by the transverse septum. The medial and lateral arcuate ligaments are thickened fascial bands that cover the anterior psoas and quadratus lumborum muscles, respectively. Note the crura and their attachments to upper lumbar vertebral bodies.

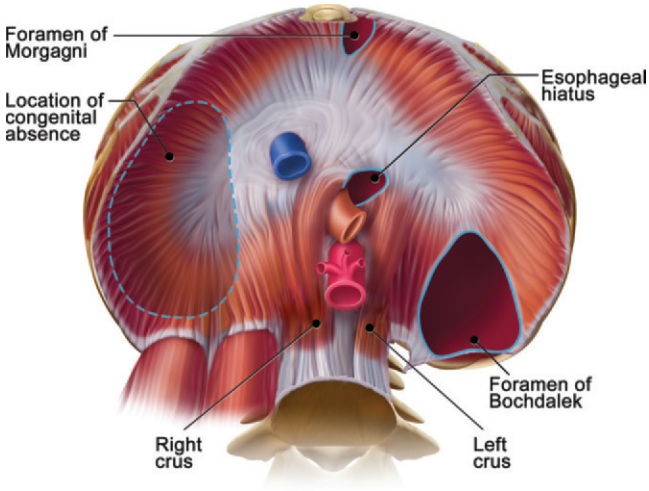

Figure 3. Drawing shows the locations of diaphragmatic hernias.

we describe treatment options for diaphragmatic dysfunction, including plication and phrenic nerve stimulation.

Embryology

The diaphragm develops during weeks 4–12 of embryogenesis. It is composed of four components: the transverse septum, pleuroperitoneal folds, esophageal mesentery, and muscular body wall (Fig 1).

The transverse septum, which is anterior, becomes the central tendon of the diaphragm (Fig 2). A defect in fusion of the transverse septum to the lateral body wall leads to an anterior (Morgagni) hernia (1) (Figs 3, 4). Morgagni hernias constitute fewer than 10% of congenital diaphragmatic hernias (2). The transverse septum fuses laterally with the muscular body wall and posteriorly with the esophageal mesentery and pleuroperitoneal folds.

Teaching Point

Teaching Point

A posterior (Bochdalek) hernia likely represents a developmental defect of the pleuroperitoneal folds or failure of fusion of the folds and transverse septum with the intercostal muscles (1) (Fig 5). Bochdalek hernias constitute 90% of congenital diaphragmatic hernias and are more common on the left side (1).

Anatomy

Attachments

The diaphragm has multiple attachments to the body wall. The two diaphragmatic crura attach the diaphragm posteriorly to the upper lumbar vertebral bodies and disks. The crura are joined by a fibrous median arcuate ligament (3). Hypertrophy or low position of this ligament can cause compression of the celiac artery, leading to epigastric pain and weight loss in median arcuate ligament syndrome (4,5) (Fig 6).

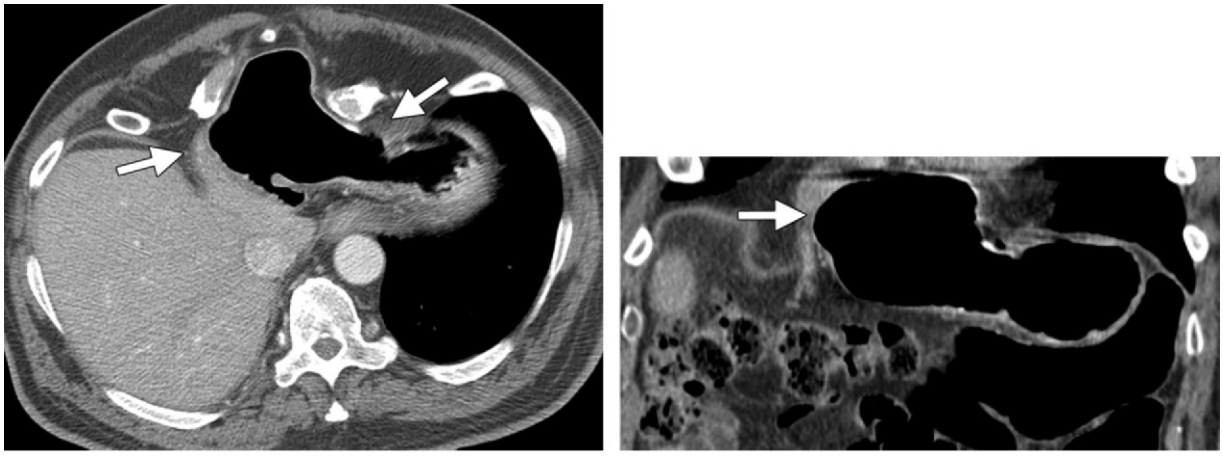

a. b.

Figure 4. Large Morgagni hernia involving the anterior right hemidiaphragm. Axial **(a)** and coronal **(b)** computed tomographic (CT) images show herniation of the stomach (arrows) through a diaphragmatic defect into both the right and left hemithoraces. Morgagni hernia results from a defect in fusion of the transverse septum to the lateral body wall.

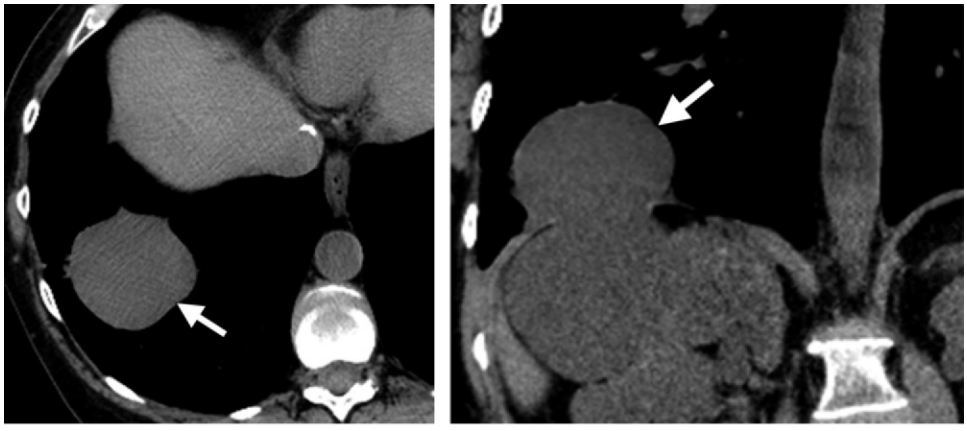

a. b.

Figure 5. Bochdalek hernia containing a renal cyst in a patient with autosomal dominant polycystic kidney disease. Axial **(a)** and coronal **(b)** CT images show a right Bochdalek hernia containing a renal cyst (arrow) and involving the posterior hemidiaphragm. Note the lack of hemidiaphragm at the focal defect. Bochdalek hernia is typically left sided and results from a developmental defect of the pleuroperitoneal folds or failure of fusion of the folds and transverse septum with the intercostal muscles.

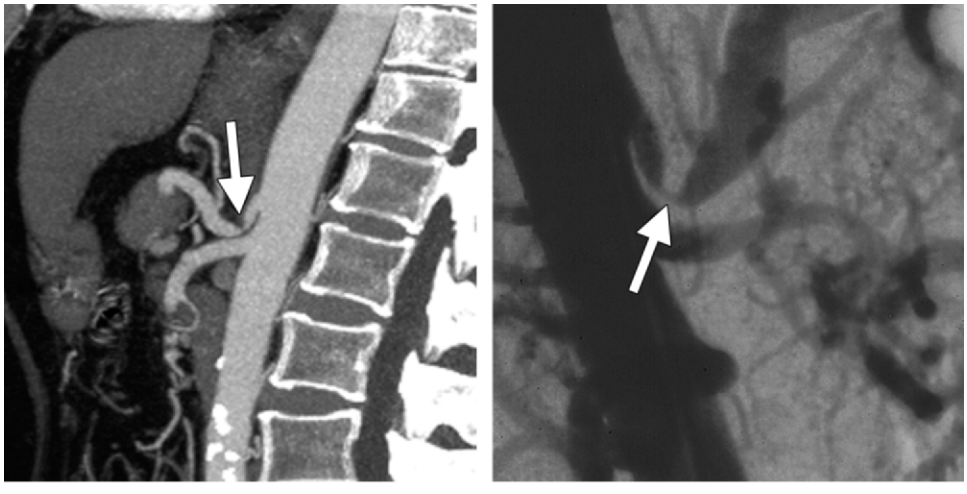

a. b.

Figure 6. Median arcuate ligament syndrome. Sagittal maximum intensity projection CT image **(a)** and oblique sagittal aortogram **(b)** show compression of the proximal celiac artery (arrow) by a low-lying and hypertrophied median arcuate ligament. (Case courtesy of Francis Scholz, MD, Lahey Clinic, Burlington, Mass.)

Figure 7. Normal lateral arcuate ligament. Coronal **(a)** and axial **(b)** CT images show the right lateral arcuate ligament (arrow) coursing to the 12th rib. This normal structure may be mistaken for lymphadenopathy or a metastatic implant.

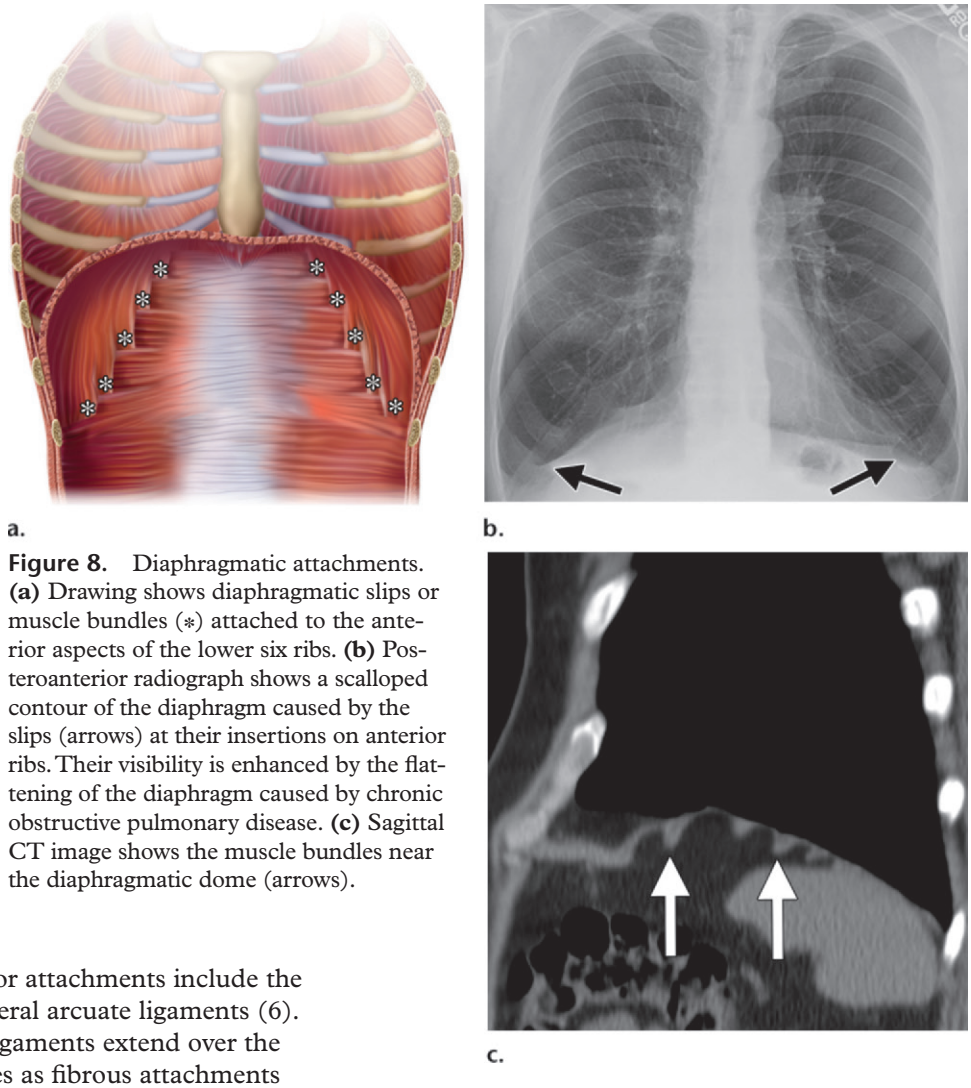

Figure 8. Diaphragmatic attachments. **(a)** Drawing shows diaphragmatic slips or muscle bundles (*) attached to the anterior aspects of the lower six ribs. **(b)** Posteroanterior radiograph shows a scalloped contour of the diaphragm caused by the slips (arrows) at their insertions on anterior ribs. Their visibility is enhanced by the flattening of the diaphragm caused by chronic obstructive pulmonary disease. **(c)** Sagittal CT image shows the muscle bundles near the diaphragmatic dome (arrows).

Additional posterior attachments include the paired medial and lateral arcuate ligaments (6). The medial arcuate ligaments extend over the anterior psoas muscles as fibrous attachments between the L1 or L2 vertebral body and the transverse processes of L1. The lateral arcuate ligaments are thickened fascial bands covering the quadratus lumborum muscle and extend from the transverse processes of T12 laterally to the midportion of the 12th ribs. The arcuate ligaments may be visible at CT and should not be mistaken for lymphadenopathy or metastatic implants (7) (Fig 7).

Anterior and lateral attachments include the inferior sternum, xiphoid process, lower six ribs, and costal cartilage (8). Diaphragmatic slips or muscle bundles may be seen attaching to anterior ribs at CT (9,10) (Fig 8).

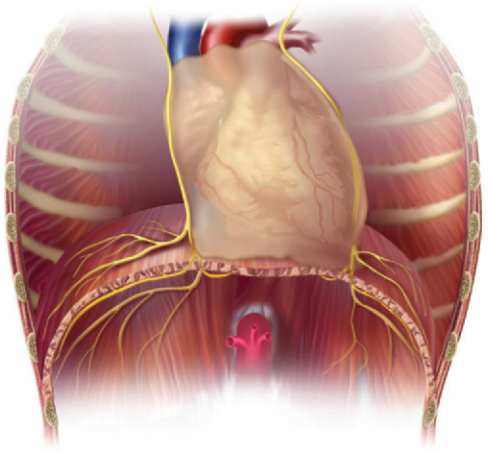

Figure 9. Course of the phrenic nerves. **(a)** Drawing shows the paired phrenic nerves (yellow), which originate from spinal nerves C3–C5 and travel through the neck and mediastinum to reach the diaphragm, where they arborize on the superior and inferior surfaces. **(b–e)** Axial CT images displayed from superior **(b)** to inferior **(e)** show the expected course of the phrenic nerves. The nerves travel with the pericardiophrenic arteries and veins (arrows).

a.

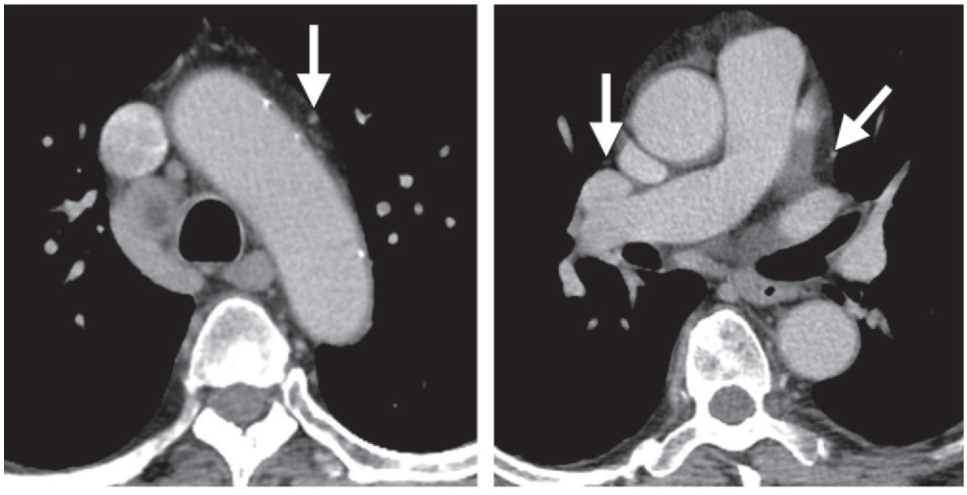

b. c.

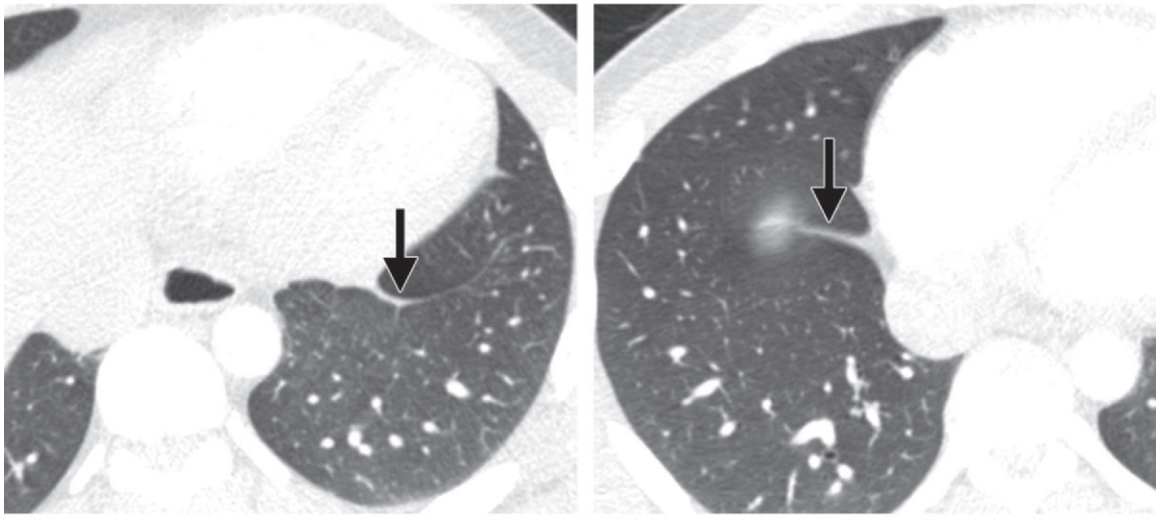

d. e.

Innervation

Innervation of the diaphragm is provided by the right and left phrenic nerves, which originate from cervical nerves C3–C5 and facilitate both sensory and motor function. The paired phrenic nerves are located posteriorly in the lateral compartment of the neck and travel anteriorly as they course through the thorax. The phrenic nerves run along the anterior surface of the pericardium before they reach the diaphragm, where they arborize on the superior and inferior surfaces (11) (Fig 9).

a.

b.

c.

Figure 10. Diaphragmatic hiatuses. **(a)** CT image shows the location of the IVC hiatus, which is at the T8 level and contains the IVC (arrow) and branches of the right phrenic nerve (not visible). It passes through the midportion of the central tendon; the actual hiatus is usually imperceptible at CT. **(b)** CT image shows the esophageal hiatus, which is at the T10 level and contains the esophagus, vagus nerve, and branches of the sympathetic plexus. It passes through the crossing of the muscle fibers of the right diaphragmatic crus (arrows), which form a ring around the esophagus. The left diaphragmatic crus (arrowhead) is also visible. **(c)** CT image shows the aortic hiatus, which is at the T12 level and contains the aorta (black arrow), thoracic duct, and hemiazygos and azygos veins. It is bordered anteriorly by the right (arrowhead) and left (white arrow) diaphragmatic crura with their attachments to the lumbar vertebral bodies.

Hiatuses

There are three main openings in the diaphragm that allow important structures to pass between the thorax and abdomen (6). The IVC hiatus is at the T8 level and contains the IVC and branches of the right phrenic nerve (Fig 10a). It passes through the midportion of the central tendon. This opening enlarges with inspiration, drawing blood into the heart.

The esophageal hiatus is at the T10 level and contains the esophagus, vagus nerve, and sympathetic nerve branches (Fig 10b). It passes through the crossing of the muscle fibers of the right diaphragmatic crus, which form a ring around

Figure 11. Diaphragmatic atrophy due to polymyositis. Coronal CT image shows thinning and elevation of both hemidiaphragms, findings that are more easily appreciated on the left (arrow).

the esophagus. This ring functions as an anatomic sphincter by constricting with inspiration and helping prevent gastroesophageal reflux.

The aortic hiatus is at the T12 level and contains the aorta, thoracic duct, and azygos and hemiazygos veins (Fig 10c). Diaphragmatic contractions do not affect this hiatus, as it is actually retrocrural.

Function

The diaphragm is the primary muscle of ventilation. During inspiration, it contracts in concert with the accessory muscles of respiration, including the external intercostal, sternocleidomastoid, and scalene muscles. This contraction expands the thoracic cavity, decreasing intrathoracic pressure and drawing air into the lungs. With relaxation of the diaphragm, the elastic recoil of the lungs predominates, causing exhalation.

In addition, the diaphragm aids in emesis, urination, and defecation by increasing intraabdominal pressure and helps prevent gastroesophageal reflux by exerting external pressure at the esophageal hiatus.

Dysfunction

Teaching Point

Dysfunction can be classified as paralysis, weakness, or eventration. It is often initially suggested by diaphragmatic elevation at chest radiography. The right hemidiaphragm is normally slightly higher than the left hemidiaphragm (12). In addition, the anterior and medial portions of the diaphragm are normally higher than the posterior and lateral portions. These findings should not be misinterpreted as signs of dysfunction.

Elevation caused by paralysis or weakness typically involves an entire hemidiaphragm, whereas elevation secondary to eventration involves only a portion of a hemidiaphragm. In diaphragmatic dysfunction, the impaired hemidiaphragm may be thinned by atrophy of the muscle (Fig 11).

Diaphragmatic dysfunction may be unilateral or, less commonly, bilateral. Unilateral impairment is often asymptomatic and discovered incidentally. Alternatively, patients can present with orthopnea or dyspnea on exertion. Symptoms are often more severe in patients with underlying pulmonary disease and may worsen when the patient is supine because of pressure from abdominal contents on the undersurface of the diaphragm (13). Pulmonary function tests show a restrictive pattern, which manifests as a reduction in forced vital capacity and forced expiratory volume in 1 second (14).

In contrast to unilateral impairment, bilateral diaphragmatic dysfunction is usually symptomatic and may lead to ventilatory failure (13). In this situation, the accessory muscles of respiration must assume all the work of breathing.

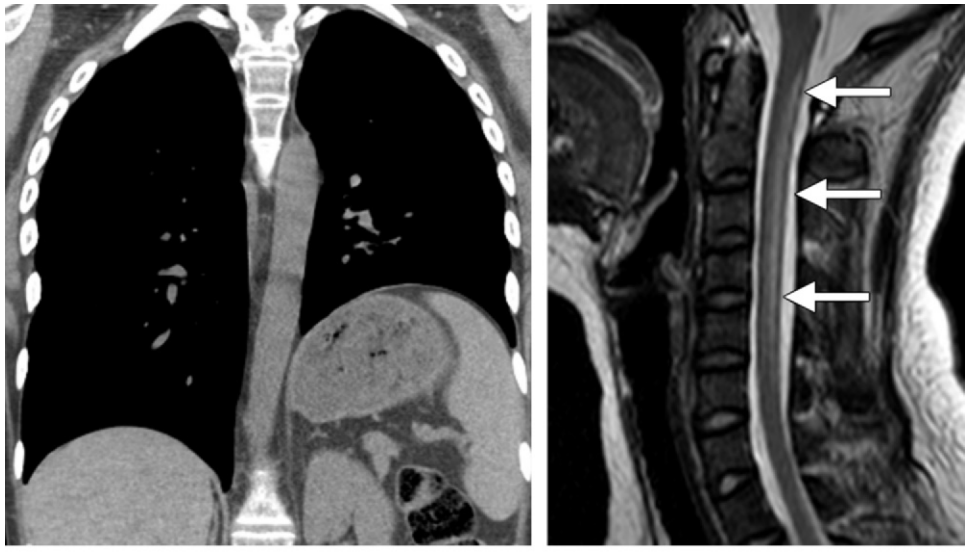

a. b.

Figure 12. Diaphragmatic dysfunction caused by transverse myelitis or leukemic infiltration of the cervical spinal cord in a patient with leukemia and shortness of breath. **(a)** Coronal CT image shows elevation of the left hemidiaphragm. **(b)** Sagittal T2-weighted MR image shows abnormal high signal intensity involving the dorsal columns (arrows). There was also focal enhancement at the C2 level (not shown). The findings are indicative of transverse myelitis or leukemic infiltration as the cause of phrenic nerve dysfunction.

Paralysis and Weakness

There are many causes of weakness and paralysis of the diaphragm; these involve the entire neuromuscular axis (see also Table E1) (15,16).

Central nervous system causes of diaphragmatic dysfunction include cervical spine trauma (17) and degeneration (18). Less commonly, cervical spinal cord disease such as transverse myelitis, syrinx, and tumor may result in paralysis or weakness (Fig 12). Dysfunction may also be due to disease of the anterior horn cells of the spinal cord, such as amyotrophic lateral sclerosis (19), poliomyelitis (20), and infection with West Nile virus (21).

Phrenic nerve dysfunction is commonly caused by cardiac surgery, which leads to diaphragmatic paralysis in 2%–20% of patients (13,22,23). One mechanism of injury is "phrenic frostbite," in which cold cardioplegia for coronary bypass or valvular surgery stuns the phrenic nerve (24). Another common cause of phrenic nerve dysfunction is direct invasion by tumor (25,26) (Figs 13, 14). Phrenic nerve neuropathies from infectious (eg, herpes zoster [27], Lyme disease [28]), immunologic (eg, Guillain-Barré syndrome [29]), or metabolic (eg, diabetes [30]) causes may also result in diaphragmatic dysfunction. Finally, radiation therapy has been implicated in phrenic nerve dysfunction (31).

Disorders of neuromuscular transmission, including myasthenia gravis and Lambert-Eaton syndrome, can also result in diaphragmatic paralysis or weakness (32). Finally, myopathies that may impair diaphragmatic function include muscular dystrophies and metabolic or immunologic disorders.

Diaphragmatic paralysis and weakness may be temporary or permanent, depending on the cause.

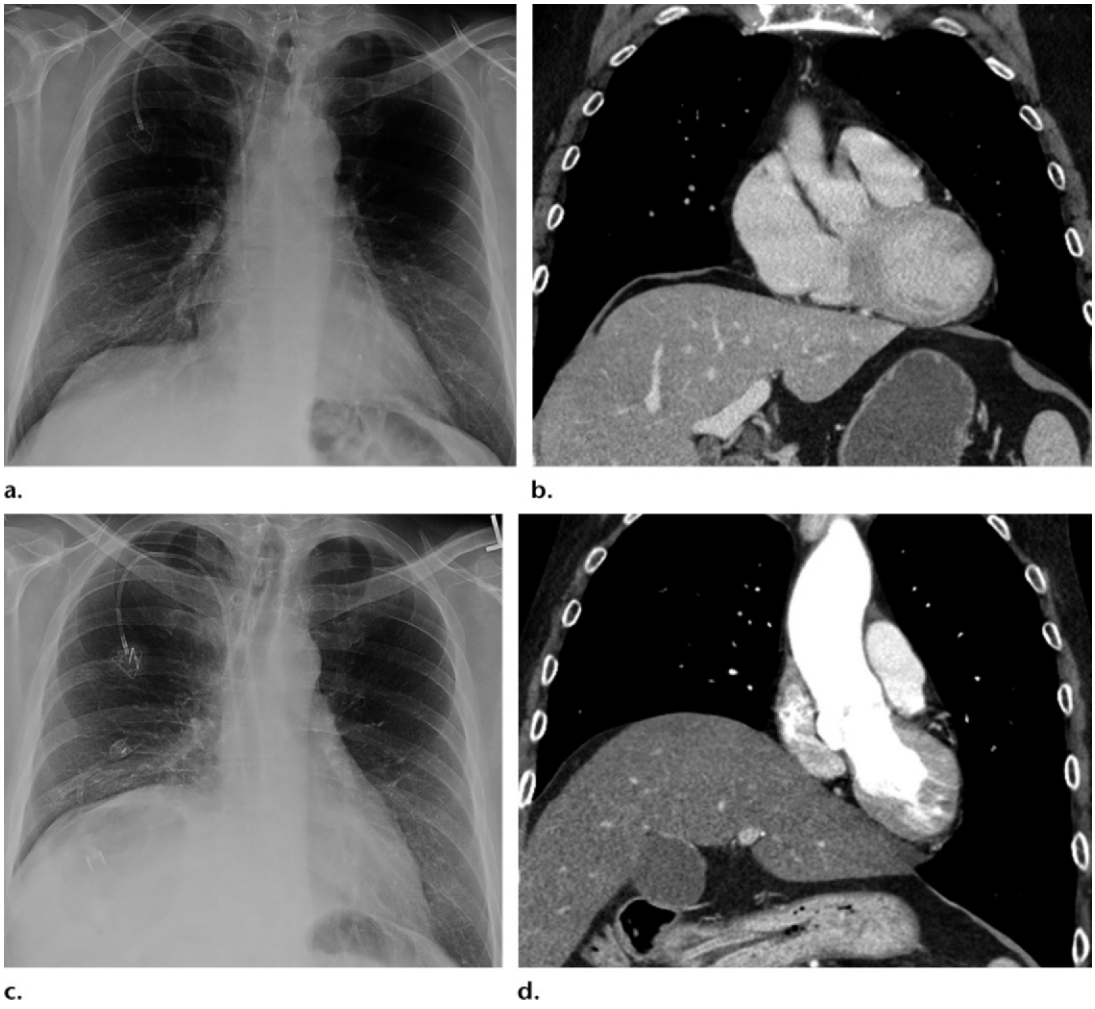

Figure 13. Diaphragmatic dysfunction due to recurrent laryngeal cancer. **(a, b)** Posteroanterior radiograph **(a)** and coronal CT image **(b)** show relatively normal height of both hemidiaphragms. **(c)** Subsequent posteroanterior radiograph shows new elevation of the right hemidiaphragm, a finding that reflects phrenic nerve dysfunction caused by recurrent malignancy. **(d)** Coronal CT image shows elevation and atrophy of the right hemidiaphragm.

Figure 14. Diaphragmatic paralysis caused by invasion of the phrenic nerve by non–small cell lung carcinoma. Coronal CT image shows elevation of the right hemidiaphragm and a right mediastinal mass (arrow).

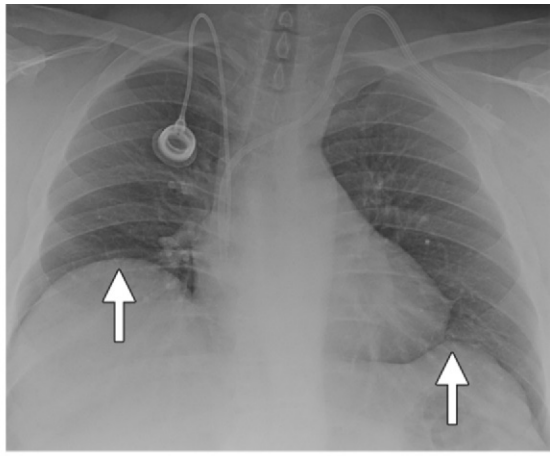

a.

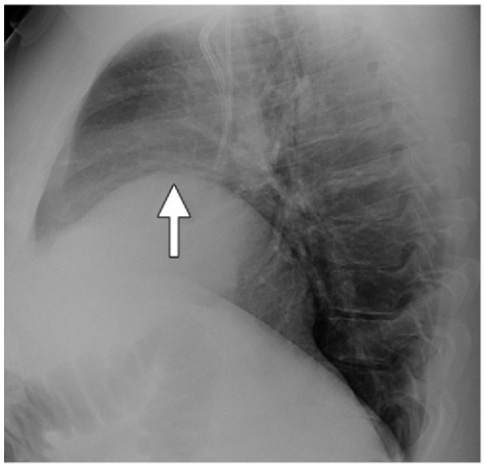

b.

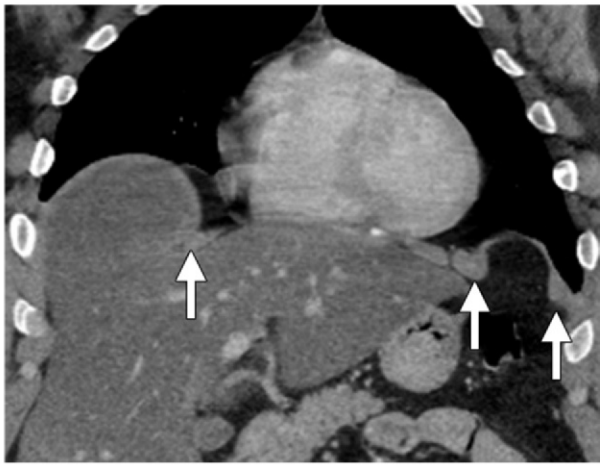

c.

Figure 15. Bilateral eventration. **(a, b)** Posteroanterior **(a)** and lateral **(b)** radiographs show focal anterior elevation of the right and left hemidiaphragms (arrows). **(c)** Coronal CT image shows focal elevation of both hemidiaphragms with undercut edges (arrows) or a mushroom appearance. Although the mushroom appearance can also occur with diaphragmatic hernia, the diaphragm in eventration is continuous.

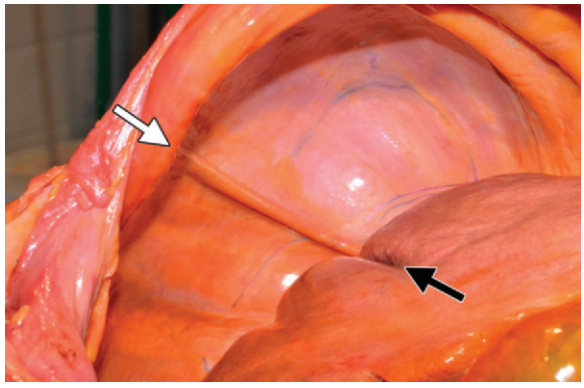

Figure 17. Eventration. Pathologic photograph shows the medial (white arrow) and lateral muscle bands of the right hemidiaphragm with a corresponding groove in the liver (black arrow). At CT, the medial muscle band formed the sharp edge of an eventration.

Eventration

Teaching Point

Eventration is a congenital thinning of the diaphragmatic muscle that causes a focal bulge. This process usually involves only a segment of a hemidiaphragm, most commonly the anteromedial portion of the right hemidiaphragm (10). On radiographs, a portion of the hemidiaphragm is elevated while the remaining portion is of normal height. At CT, there may be a sharp transition at the edge of the eventration (Figs 15–17; see also Movie 1). Sometimes the edges are undercut with ballooning above. Eventration can usually be distinguished from paralysis at radiography (33) and CT, although it can be mistaken for diaphragmatic hernia.

Eventration can become more pronounced with increasing intraabdominal pressure, usually as a result of abdominal obesity (Fig 18).

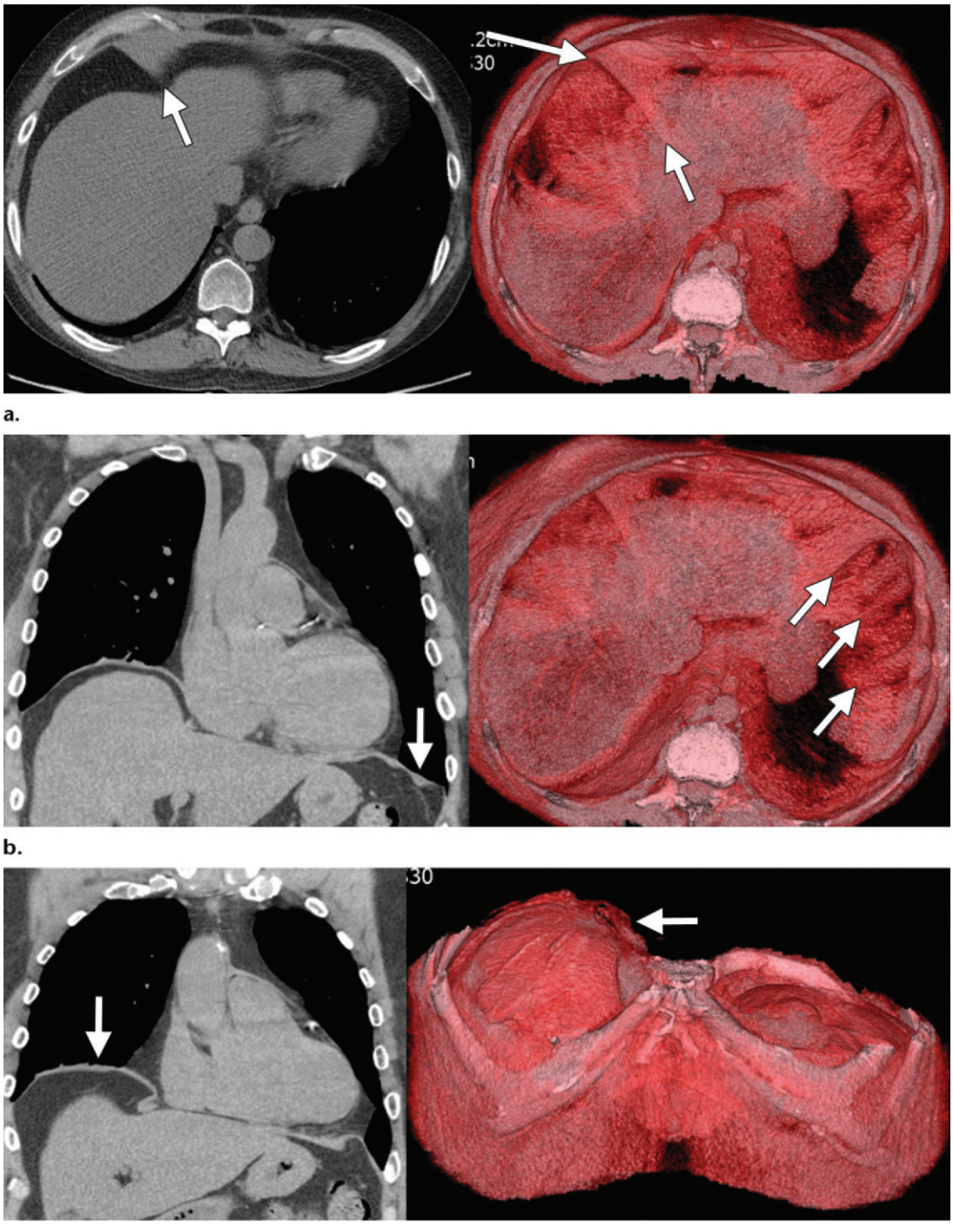

Figure 16. Eventration of the right hemidiaphragm. **(a)** Axial (left) and three-dimensional (3D) volume-rendered (right) CT images show eventration of the edge of the right hemidiaphragm (arrows). Note the abrupt margin and the impression on the surface of the liver. **(b)** Coronal (left) and 3D volume-rendered (right) CT images show normal left diaphragmatic muscle bundles (arrows). **(c)** Coronal (left) and 3D volume-rendered (right) CT images show right hemidiaphragmatic eventration (arrows).

Figure 18. Enlargement of eventration by increased abdominal pressure due to fat or ascites. **(a, b)** Initial posteroanterior **(a)** and lateral **(b)** radiographs show mild focal anterior elevation of the right hemidiaphragm (arrow). **(c, d)** Posteroanterior **(c)** and lateral **(d)** radiographs in the same patient after liver transplantation and weight gain show increased elevation of the right hemidiaphragm (arrow) owing to abdominal obesity. **(e)** Coronal CT image in a patient with ascites shows exaggerated eventration of the right hemidiaphragm with an undercut edge (mushroom appearance) (arrow).

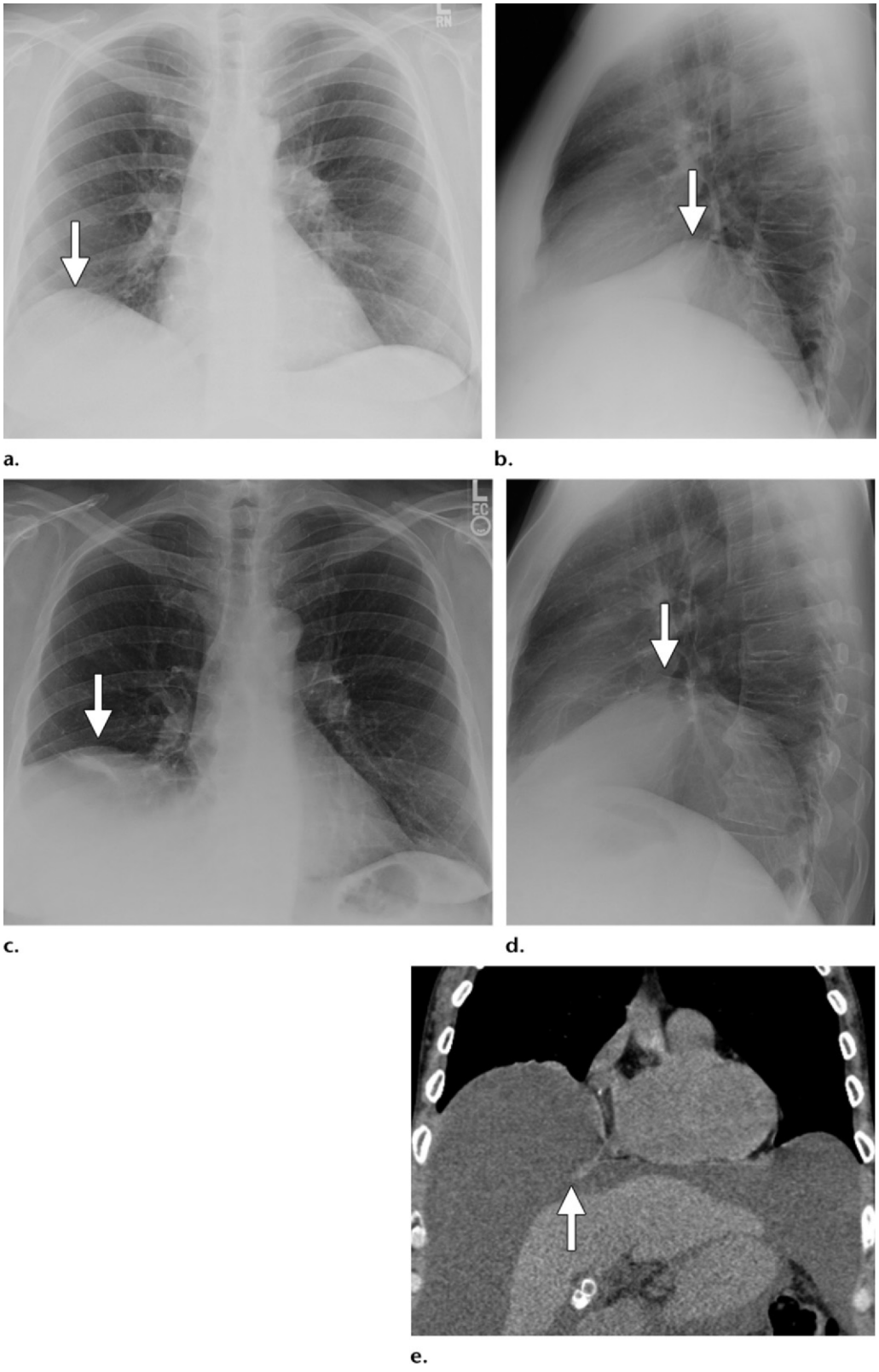

Figure 19. Diaphragmatic elevation due to normal exhalation. **(a)** Normal inspiratory posteroanterior radiograph shows a minimal height difference between the hemidiaphragms. The right hemidiaphragm is normally slightly higher than the left. **(b)** Normal expiratory posteroanterior radiograph obtained at the same time shows that both hemidiaphragms have moved cranially by more than one rib interspace. Lung volumes have decreased with new basal atelectasis.

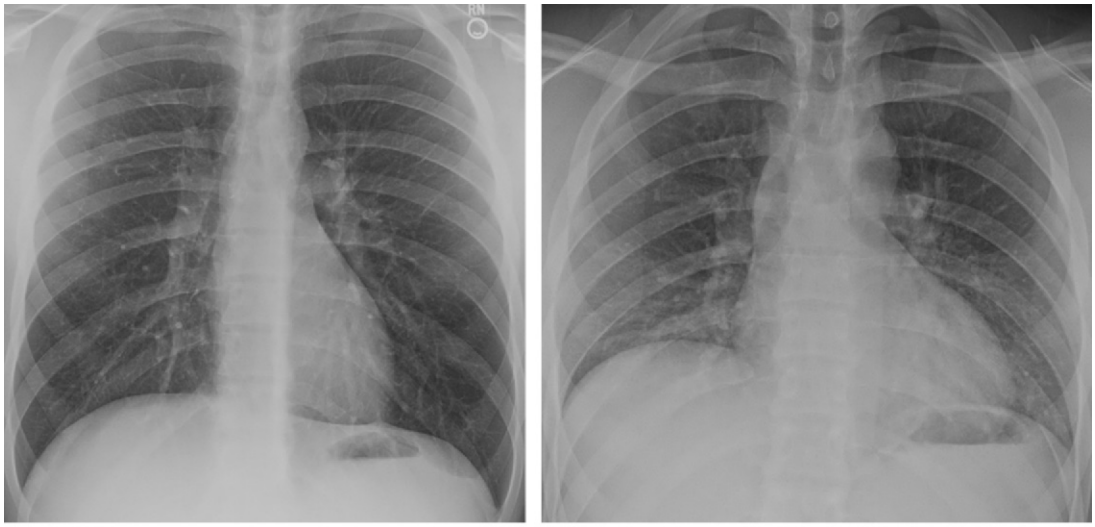

a. b.

Figure 20. Diaphragmatic elevation secondary to pulmonary fibrosis. **(a)** Initial posteroanterior radiograph shows elevation of both hemidiaphragms (arrows) owing to advanced pulmonary fibrosis. **(b)** On a radiograph obtained after transplantation of the left lung, the left hemidiaphragm is lower but the right hemidiaphragm remains elevated (arrow). This elevation should not be misinterpreted as indicative of right phrenic nerve injury.

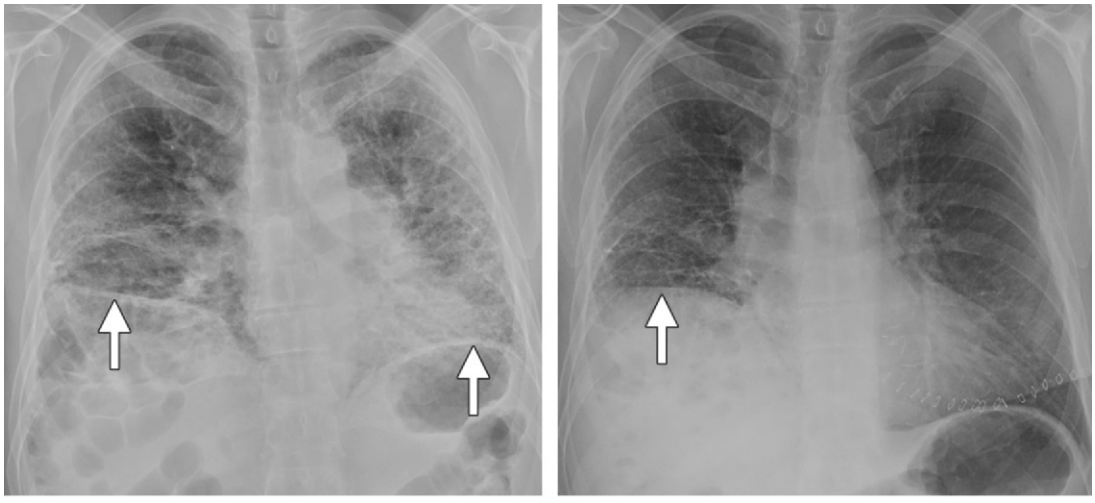

a. b.

Mimics

Diaphragmatic elevation can also be caused by other conditions, including normal exhalation (Fig 19). Any process that increases intraabdominal pressure, including abdominal obesity, ascites, and hepatosplenomegaly, may cause elevation of the diaphragm. Conversely, conditions that cause lung volume loss may pull the diaphragm superiorly, causing elevation. These conditions include atelectasis, lung resection, and pulmonary fibrosis (Fig 20).

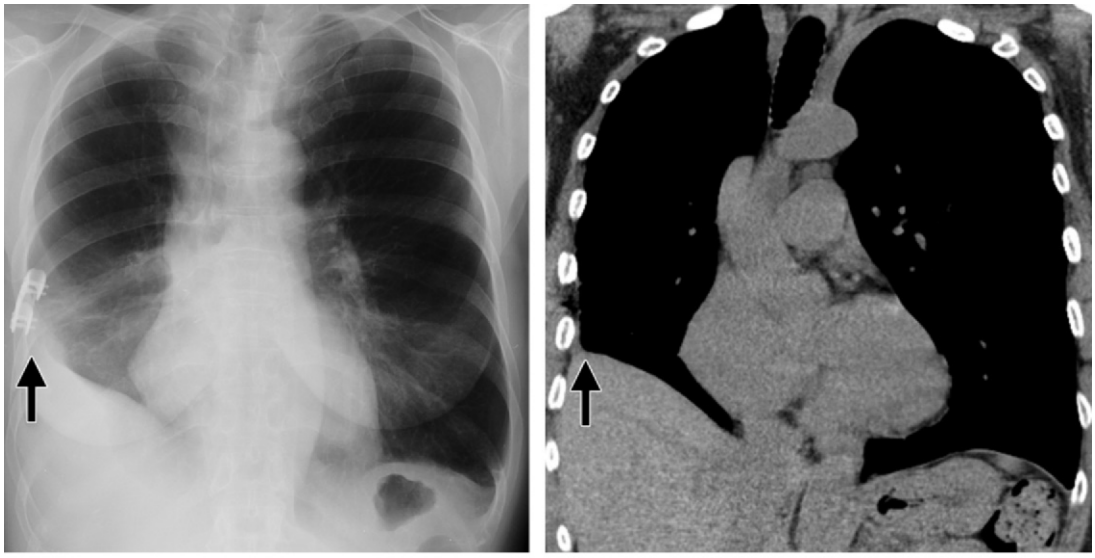

a. b.

Figure 21. Tethering of the diaphragm after resection of the right lower lobe. Posteroanterior radiograph **(a)** and coronal CT image **(b)** show tethering of the right hemidiaphragm (arrow) to the lateral chest wall owing to pleural thickening.

In patients with pleural thickening, the diaphragm may become tethered to the chest wall, causing elevation and an abnormal diaphragmatic contour (Fig 21). Subpulmonic pleural effusion mimics diaphragmatic elevation, but the relatively flat appearance and lateral peaking of the apparent dome should suggest a subpulmonic effusion rather than elevation of the hemidiaphragm (34) (Fig 22).

Fluoroscopic Sniff Test

Functional imaging allows further evaluation after diaphragmatic elevation is recognized on a radiograph. Most often, we use the fluoroscopic sniff test to evaluate function of the diaphragm. This examination is simple to perform and the results are easy to interpret.

Technique

Before fluoroscopy, we have the patient practice deep breathing (with the mouth open) and sniffing. For sniffing, we tell the patient to first take in a deep breath, then breathe all the way out, and finally (with the mouth closed) to breathe in as hard, fast, and deeply as possible. We have the patient practice this twice.

With the fluoroscopy table vertical, we have the patient stand on the platform with his or her back against the table. We center the x-ray beam at the level of the diaphragm and collimate from the sides. However, we include the upper chest so that we can observe the motion of the anterior chest wall.

We observe and record two or three quiet (spontaneous and uninstructed) breaths and then two or three deep breaths and finally two or three sniffs. Then we have the patient rotate into the lateral position with arms raised or folded on top of the head and repeat the sequence of quiet breaths, deep breaths, and sniffs. Imaging in the lateral position shows the motion of the posterior hemidiaphragms, which may move differently from the anterior hemidiaphragms. It also shows the motion of the sternum and anterior chest wall.

With each breath and sniff, we observe the direction of motion and the extent of excursion of each hemidiaphragm relative to the contralateral hemidiaphragm and rib cage. We record video loops into the picture archiving and communication system and usually also onto a digital video disc.

Normal Findings

On quiet and deep inspiration, both hemidiaphragms move downward as the anterior chest wall moves upward (see also Movies 2 and 3). On deep inspiration, normal excursion is at least one rib interspace in adults. The excursion may be somewhat asymmetric and there may be a slight delay or lag on one side, typically the right (35). In the lateral projection, the excursion of the posterior part of the hemidiaphragm may be greater than that of the anterior part, especially on the right.

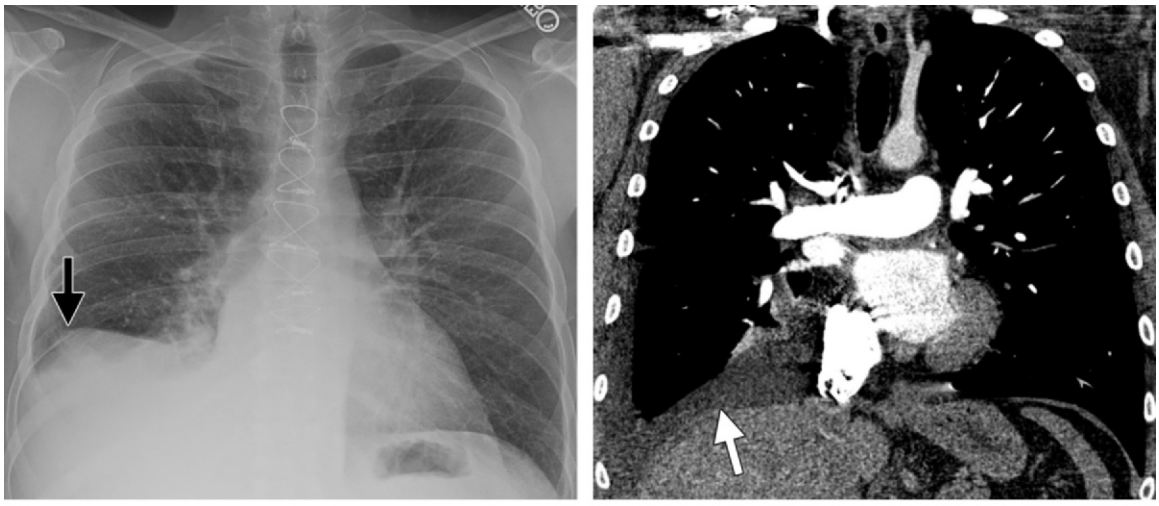

a. b.

Figure 22. Subpulmonic pleural effusion mimicking hemidiaphragmatic elevation. **(a)** Posteroanterior radiograph shows an appearance that was initially interpreted as elevation of the right hemidiaphragm. Close inspection reveals a lateral peak (arrow), a finding suggestive of a subpulmonic effusion. **(b)** Coronal CT image shows a subpulmonic effusion (arrow). The right hemidiaphragm has a normal position.

On sniffing, both hemdiaphragms move downward. The anterior chest wall may not initially move upward as much as on slow deep inspiration. As on deep inspiration, there may be some asymmetry of excursion, there may be a slight lag on one side, and the motion of the posterior aspect of the hemidiaphragm may be more vigorous than that of the anterior part, especially on the right. If sniffing is very vigorous, there can even be momentary slight paradoxical (upward) motion of the anterior hemidiaphragm, particularly the right.

Abnormal Findings

In paralysis of one hemidiaphragm, orthograde excursion is absent and there may be paradoxical motion even on quiet and deep inspiration (see also Movies 4 and 5). On sniffing, there is usually paradoxical motion.

In paralysis of both hemidiaphragms, the two may move paradoxically together if anterior chest wall motion is vigorous enough (see also Movie 6). This symmetric motion of the two hemidiaphragms may at first appear to be normal until the radiologist recognizes that the hemidiaphragms are passively following the anterior ribs upward on inspiration, rather than moving in the opposite direction, as is normal.

In weakness of one or both hemidiaphragms, excursion is reduced or delayed on quiet and deep inspiration (see also Movies 7–9). If weakness is more severe, motion may be paradoxical on deep breathing and even on quiet breathing, especially anteriorly. On sniffing, motion is usually paradoxical. However, if there is any orthograde motion on quiet or deep inspiration, then the hemidiaphragm is merely weak, but not paralyzed.

Eventration of the hemidiaphragm is a special case of weakness in which only a segment of the hemidiaphragm (typically the anterior aspect on the right) moves abnormally. In this case, excursion of the affected segment is reduced on quiet and deep inspiration and may be paradoxical on sniffing (see also Movie 10). The posterior aspect of the hemidiaphragm retains normal motion. This can lead to a rocking motion of the hemidiaphragm on the lateral view, with the anterior part moving up as the posterior part moves down.

Technical Adjustments for Special Patients

Sometimes a patient becomes dyspneic or hypoxemic when lying down, and it may then be useful to supplement upright fluoroscopy with supine fluoroscopy. Normally, the diaphragm is higher and its excursion is reduced when the patient is supine, because the diaphragm has to work against the weight of the abdomen. An exaggerated decrement in lung volume or excursion of the diaphragm with the patient supine may explain the symptoms.

If the patient cannot stand for fluoroscopy, we have the patient sit in a wheelchair or lie supine on the table. Again, if the patient is supine, excursion of the diaphragm is reduced by the weight of

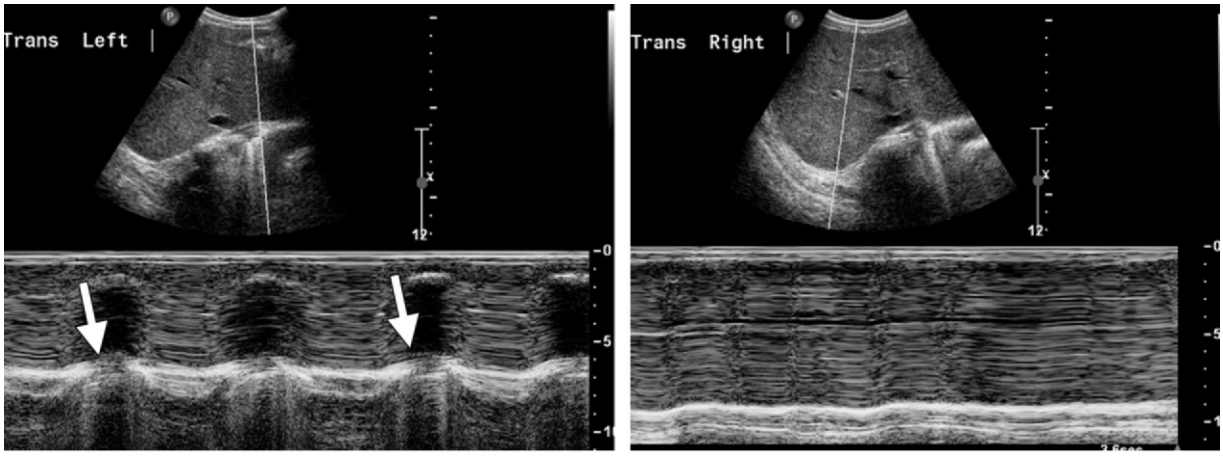

a. b.

Figure 23. Diaphragmatic paralysis in a 9-month-old infant with complex congenital heart disease who underwent a Rastelli procedure. **(a)** Longitudinal US image of the left hemidiaphragm and M-mode tracing show normal orthograde diaphragmatic motion. During inspiration, the diaphragm moves in the inferior direction (arrows), toward the transducer. **(b)** Longitudinal US image of the right hemidiaphragm and associated M-mode tracing show only minimal diaphragmatic motion. The right hemidiaphragm moved in the superior direction during inspiration, a finding indicative of paradoxical motion. These findings are consistent with paralysis of the right hemidiaphragm. (Case courtesy of Jonathan Swanson, MD, Seattle Childrens Hospital, Seattle, Wash.)

the abdomen. We do not normally include lateral fluoroscopy if the patient cannot stand or sit.

If the patient undergoes fluoroscopy to explain ventilator dependence, we observe the motion of the diaphragm with the ventilator attached and then work with the respiratory therapist to briefly disconnect the ventilator and record a few spontaneous deep breaths before resuming mechanical ventilation. In this setting, we do not attempt sniffing or lateral views.

If a patient has a tracheostomy tube but is able to breathe on his or her own and to cooperate, we can replicate sniffing by having the patient use a finger to partly occlude the tracheostomy tube during forceful inspiration.

US and MR Imaging

Diaphragmatic US has the benefit of portability and is often considered the preferred examination in children and young adults owing to the absence of ionizing radiation. At US, the diaphragm appears as a thick echogenic line. M-mode US may be used to measure the direction of diaphragmatic motion and the amplitude of excursion (36–38) (Fig 23).

Although the method of observation is different and the examination may or may not be performed with sniffing, the concept behind this examination is identical to that of the fluoroscopic sniff test. Normal hemidiaphragms move inferiorly with inhalation. There is similar excursion of the two hemidiaphragms, although the motion of the left hemidiaphragm may be slightly greater than that of the right hemidiaphragm (see also Movie 11). A paralyzed hemidiaphragm will demonstrate no orthograde movement with quiet breathing and may have paradoxical movement (see also Movie 12).

Although not yet widely used in practice, performance of dynamic MR imaging for evaluation of diaphragmatic function has also been described (39–41). Spoiled gradient-echo and cine balanced steady-state free-precession sequences may be used. Quantitative evaluation with MR imaging may allow assessment of the excursion, synchronicity, and velocity of diaphragmatic motion. This modality also has the advantage of no ionizing radiation, but use of MR imaging for functional imaging of the diaphragm is largely limited by high costs.

Treatment

There are various treatment options for diaphragmatic dysfunction; the choice depends on the severity and cause of the dysfunction. Most patients with unilateral diaphragmatic dysfunction

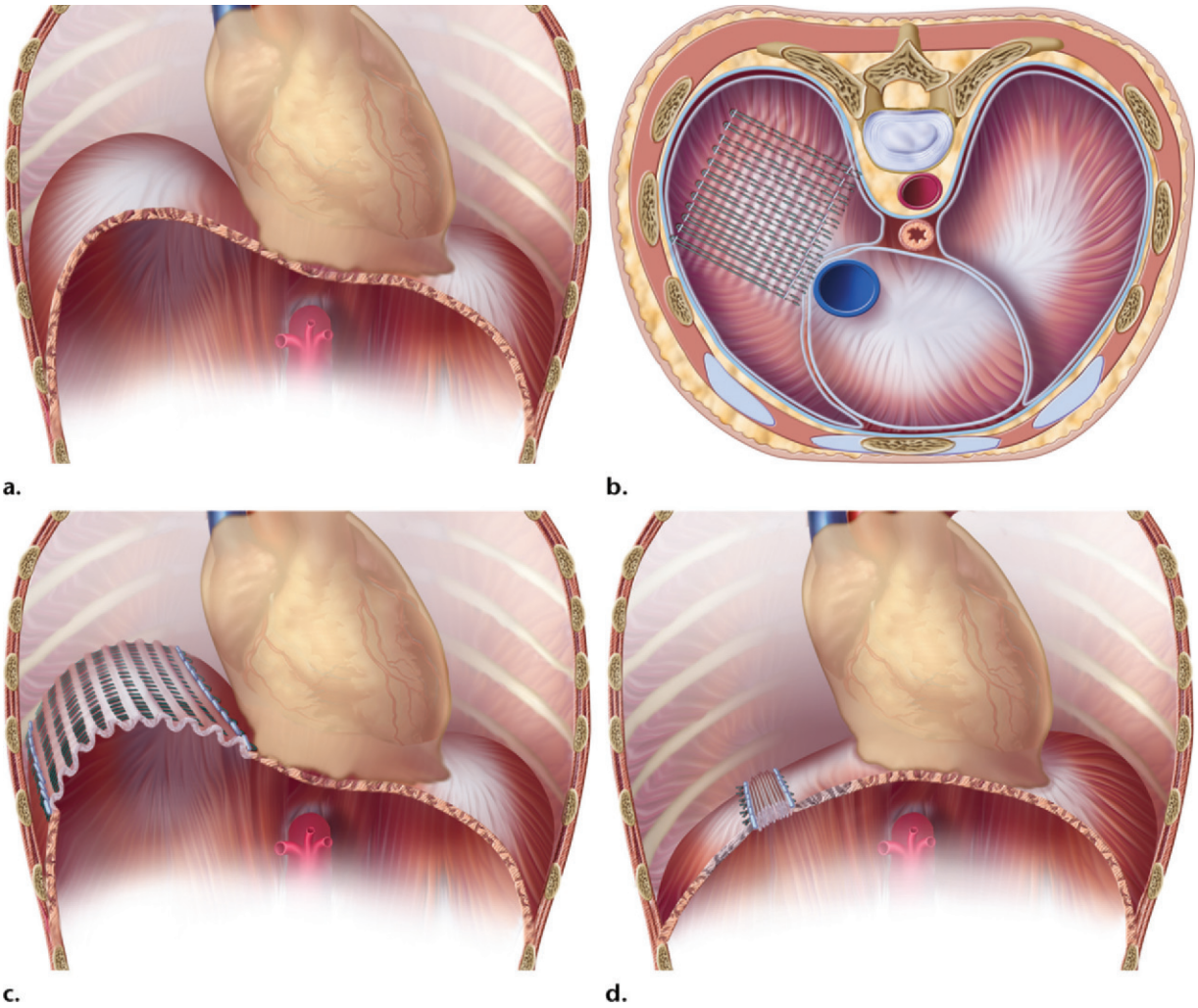

Figure 24. Diaphragmatic plication. **(a)** Drawing (frontal view) shows an elevated right hemidiaphragm, such as might be caused by a phrenic nerve injury. **(b, c)** Drawings (view from above [**b**] and frontal view [**c**]) show initial placement of sutures buttressed by Teflon pledgets, thus forming pleats in the hemidiaphragm. **(d)** Drawing (frontal view) shows the pleats pulled together, lowering and tightening the hemidiaphragm and increasing intrathoracic volume. (This technique is the one used by Michael S. Mulligan, MD, University of Washington, Seattle, Wash, who supervised these drawings.)

are asymptomatic, and conservative management is indicated. Patients with bilateral diaphragmatic paralysis are typically the most symptomatic and often require long-term positive-pressure ventilation.

Plication

For symptomatic patients in whom phrenic nerve injury is believed to be irreversible, plication of the hemidiaphragm may be considered. In adults, a waiting period of at least 1 year is often implemented. In children, surgery is typically performed soon after diagnosis, since diaphragmatic dysfunction is less well tolerated and plication may allow weaning from mechanical ventilation (42).

Diaphragmatic plication is traditionally performed by means of thoracotomy, although minimally invasive transabdominal and transthoracic techniques have also been described (43). The thinned and flaccid muscle and central tendon are gathered in pleats and sutured, lowering and tightening the hemidiaphragm and increasing intrathoracic volume (Fig 24).

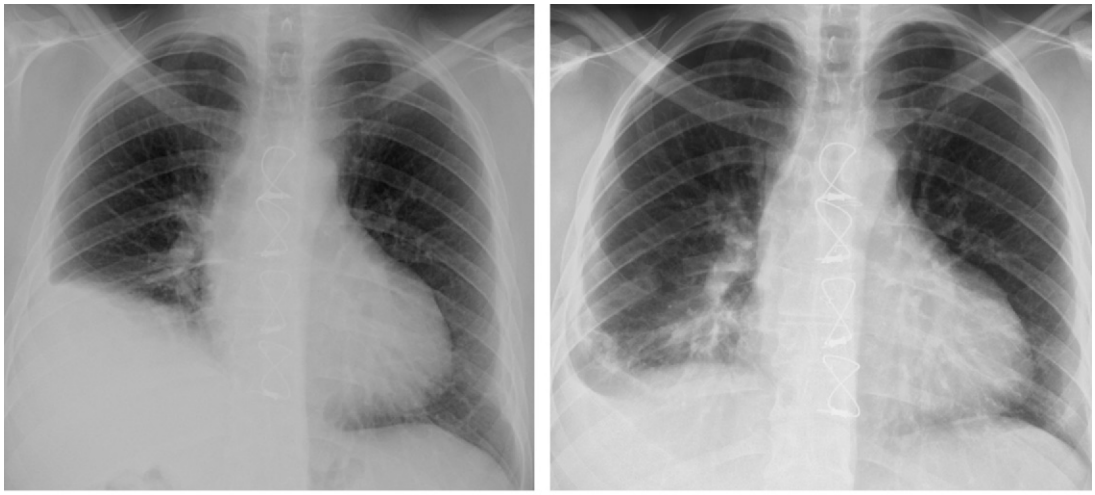

a. b.

Figure 25. Effect of diaphragmatic plication. **(a)** Initial radiograph shows elevation of the right hemidiaphragm owing to a phrenic nerve injury caused by cardiac surgery. Because of the patient's shortness of breath, plication was performed to expand intrathoracic volume. **(b)** Radiograph obtained after plication shows increased right lung volume, a finding that reflects tightening and lowering of the right hemidiaphragm.

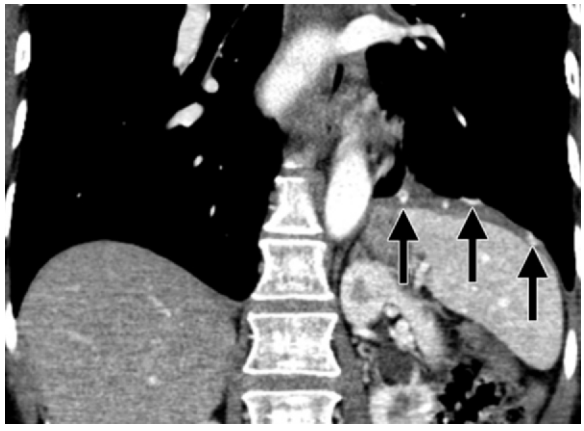

Figure 26. Diaphragmatic plication for treatment of paralysis caused by resection of a thymoma. Coronal CT image shows high-attenuation Teflon pledgets (arrows) along the surface of the left hemidiaphragm. These pledgets are used to buttress the sutures used in plication.

Although function of the hemidiaphragm is not restored, symptoms decrease and pulmonary function improves after plication (44–47). Chest imaging demonstrates decreased elevation of the affected hemidiaphragm (Fig 25). Close inspection of the diaphragm may reveal surgical pledgets used to buttress the sutures forming the diaphragmatic pleats (Fig 26).

Phrenic Nerve Stimulation

A select subset of patients may benefit from phrenic nerve stimulation. As opposed to plication, phrenic nerve stimulation has the potential advantage of restoring orthograde diaphragmatic motion. This procedure is typically reserved for patients who have intact phrenic nerve function without evidence of myopathy. In patients with high cervical spine injuries and bilateral diaphragmatic paralysis, phrenic nerve stimulation can supplant positive-pressure ventilation, with improved quality of life and greater independence (48).

A limited thoracotomy is performed, and an electrode is implanted adjacent to the phrenic nerve. The electrode is connected to a receiver unit in a subcutaneous pocket (Fig 27).

Summary

The diaphragm is the primary muscle of ventilation. Dysfunction of the diaphragm is an underappreciated cause of respiratory difficulties and may be due to a wide variety of entities, including surgery, trauma, tumor, and infection. Diaphragmatic disease usually manifests as elevation.

Functional imaging with fluoroscopy (or US or MR imaging) is a simple and effective way to

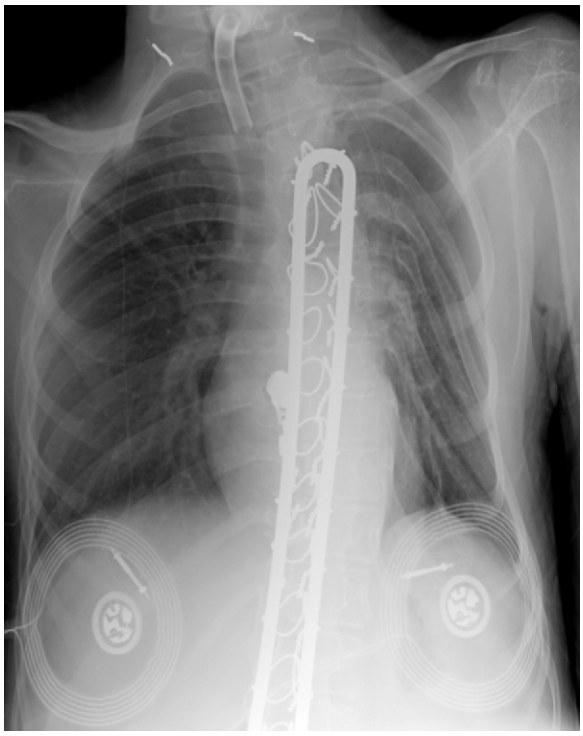

Figure 27. Phrenic nerve stimulation in a patient with C3 tetraplegia after a motor vehicle collision at 4 years of age. Posteroanterior radiograph shows bilateral phrenic nerve stimulators. After placement of the stimulators, the patient was successfully weaned from daytime mechanical ventilation.

Teaching Point

diagnose diaphragmatic dysfunction. Paralysis is indicated by absence of orthograde excursion on quiet and deep breathing, with paradoxical motion on sniffing. Weakness is indicated by reduced or delayed orthograde excursion on deep breathing, with or without paradoxical motion on sniffing. Eventration is congenital thinning of a segment of diaphragmatic muscle and manifests as focal weakness.

Treatment of diaphragmatic paralysis depends on the cause of the dysfunction and the severity of the symptoms. Plication and phrenic nerve stimulation are options.

Acknowledgment.—The authors thank Kate Sweeney of University of Washington Creative Services for the anatomic illustrations.

Disclosures of Potential Conflicts of Interest.—**C.L.F.:** *Related financial activities:* none. *Other financial activities:* consultant for Snohomish County, Washington, and for attorneys; reviewer for Autopsy: Healthwise. **C.M.W.:** *Related financial activities:* none. *Other financial activities:* royalties from Amirsys. **J.D.G.:** *Related financial activities:* consultant for Madigan Army Medical Center; reviewer for Spiration DSMB and Parexel. *Other financial activities:* none.

References

1. Taylor GA, Atalabi OM, Estroff JA. Imaging of congenital diaphragmatic hernias. Pediatr Radiol 2009; 39(1):1–16.
2. Robnett-Filly B, Goldstein RB, Sampior D, Hom M. Morgagni hernia: a rare form of congenital diaphragmatic hernia. J Ultrasound Med 2003;22(5): 537–539.
3. Shin MS, Berland LL. Computed tomography of retrocrural spaces: normal, anatomic variants, and pathologic conditions. AJR Am J Roentgenol 1985; 145(1):81–86.
4. Lindner HH, Kemprud E. A clinicoanatomical study of the arcuate ligament of the diaphragm. Arch Surg 1971;103(5):600–605.
5. Horton KM, Talamini MA, Fishman EK. Median arcuate ligament syndrome: evaluation with CT angiography. RadioGraphics 2005;25(5):1177–1182.
6. Panicek DM, Benson CB, Gottlieb RH, Heitzman ER. The diaphragm: anatomic, pathologic, and radiologic considerations. RadioGraphics 1988;8(3): 385–425.
7. Silverman PM, Cooper C, Zeman RK. Lateral arcuate ligaments of the diaphragm: anatomic variations at abdominal CT. Radiology 1992;185(1):105–108.
8. Kleinman PK, Raptopoulos V. The anterior diaphragmatic attachments: an anatomic and radiologic study with clinical correlates. Radiology 1985;155 (2):289–293.
9. Chavhan GB, Babyn PS, Cohen RA, Langer JC. Multimodality imaging of the pediatric diaphragm: anatomy and pathologic conditions. RadioGraphics 2010;30(7):1797–1817.
10. Yeh HC, Halton KP, Gray CE. Anatomic variations and abnormalities in the diaphragm seen with US. RadioGraphics 1990;10(6):1019–1030.
11. Maish MS. The diaphragm. Surg Clin North Am 2010;90(5):955–968.
12. O'Brien FW. Elevation of the diaphragm. Radiology 1928;10(3):226–233.
13. Qureshi A. Diaphragm paralysis. Semin Respir Crit Care Med 2009;30(3):315–320.
14. De Troyer A, Borenstein S, Cordier R. Analysis of lung volume restriction in patients with respiratory muscle weakness. Thorax 1980;35(8):603–610.
15. Wilcox PG, Pardy RL. Diaphragmatic weakness and paralysis. Lung 1989;167(6):323–341.
16. Billings ME, Aitken ML, Benditt JO. Bilateral diaphragm paralysis: a challenging diagnosis. Respir Care 2008;53(10):1368–1371.
17. Carter RE. Unilateral diaphragmatic paralysis in spinal cord injury patients. Paraplegia 1980;18(4): 267–274.
18. Hayashi H, Kihara S, Hoshimaru M, Hashimoto N. Diaphragmatic paralysis caused by cervical spondylosis: case report. J Neurosurg Spine 2005;2(5): 604–607.
19. Evangelista T, Carvalho M, Pinto A, de Lurdes Sales Luís M. Phrenic nerve conduction in amyotrophic lateral sclerosis. J Neurol Sci 1995;129(suppl): 35–37.

20. Lane DJ, Hazleman B, Nichols PJR. Late onset respiratory failure in patients with previous poliomyelitis. Q J Med 1974;43(172):551–568.
21. Betensley AD, Jaffery SH, Collins H, Sripathi N, Alabi F. Bilateral diaphragmatic paralysis and related respiratory complications in a patient with West Nile virus infection. Thorax 2004;59(3):268–269.
22. Dorffner R, Eibenberger K, Youssefzadeh S, et al. Diaphragmatic dysfunction after heart or lung transplantation. J Heart Lung Transplant 1997;16(5):566–569.
23. Dimopoulou I, Daganou M, Dafni U, et al. Phrenic nerve dysfunction after cardiac operations: electrophysiologic evaluation of risk factors. Chest 1998;113(1):8–14.
24. Olopade CO, Staats BA. Time course of recovery from frostbitten phrenics after coronary artery bypass graft surgery. Chest 1991;99(5):1112–1115.
25. Piehler JM, Pairolero PC, Gracey DR, Bernatz PE. Unexplained diaphragmatic paralysis: a harbinger of malignant disease? J Thorac Cardiovasc Surg 1982;84(6):861–864.
26. Gibson GJ. Diaphragmatic paresis: pathophysiology, clinical features, and investigation. Thorax 1989;44(11):960–970.
27. Derveaux L, Lacquet LM. Hemidiaphragmatic paresis after cervical herpes zoster. Thorax 1982;37(11):870–871.
28. Abbott RA, Hammans S, Margarson M, Aji BM. Diaphragmatic paralysis and respiratory failure as a complication of Lyme disease. J Neurol Neurosurg Psychiatry 2005;76(9):1306–1307.
29. Durand MC, Prigent H, Sivadon-Tardy V, et al. Significance of phrenic nerve electrophysiological abnormalities in Guillain-Barré syndrome. Neurology 2005;65(10):1646–1649.
30. White JE, Bullock RE, Hudgson P, Home PD, Gibson GJ. Phrenic neuropathy in association with diabetes. Diabet Med 1992;9(10):954–956.
31. Brander PE, Järvinen V, Lohela P, Salmi T. Bilateral diaphragmatic weakness: a late complication of radiotherapy. Thorax 1997;52(9):829–831.
32. Gilchrist JM. Overview of neuromuscular disorders affecting respiratory function. Semin Respir Crit Care Med 2002;23(3):191–200.
33. Verhey PT, Gosselin MV, Primack SL, Kraemer AC. Differentiating diaphragmatic paralysis and eventration. Acad Radiol 2007;14(4):420–425.
34. Rothstein E, Landis FB. Infrapulmonary pleural effusion simulating elevation of the hemidiaphragm. Am J Med 1950;8(1):46–52.
35. Alexander C. Diaphragm movements and the diagnosis of diaphragmatic paralysis. Clin Radiol 1966;17(1):79–83.
36. Gerscovich EO, Cronan M, McGahan JP, Jain K, Jones CD, McDonald C. Ultrasonographic evaluation of diaphragmatic motion. J Ultrasound Med 2001;20(6):597–604.
37. Epelman M, Navarro OM, Daneman A, Miller SF. M-mode sonography of diaphragmatic motion: description of technique and experience in 278 pediatric patients. Pediatr Radiol 2005;35(7):661–667.
38. Lloyd T, Tang YM, Benson MD, King S. Diaphragmatic paralysis: the use of M mode ultrasound for diagnosis in adults. Spinal Cord 2006;44(8):505–508.
39. Gierada DS, Curtin JJ, Erickson SJ, Prost RW, Strandt JA, Goodman LR. Diaphragmatic motion: fast gradient-recalled-echo MR imaging in healthy subjects. Radiology 1995;194(3):879–884.
40. Unal O, Arslan H, Uzun K, Ozbay B, Sakarya ME. Evaluation of diaphragmatic movement with MR fluoroscopy in chronic obstructive pulmonary disease. Clin Imaging 2000;24(6):347–350.
41. Kiryu S, Loring SH, Mori Y, Rofsky NM, Hatabu H, Takahashi M. Quantitative analysis of the velocity and synchronicity of diaphragmatic motion: dynamic MRI in different postures. Magn Reson Imaging 2006;24(10):1325–1332.
42. Simansky DA, Paley M, Refaely Y, Yellin A. Diaphragm plication following phrenic nerve injury: a comparison of paediatric and adult patients. Thorax 2002;57(7):613–616.
43. Groth SS, Andrade RS. Diaphragm plication for eventration or paralysis: a review of the literature. Ann Thorac Surg 2010;89(6):S2146–S2150.
44. Groth SS, Rueth NM, Kast T, et al. Laparoscopic diaphragmatic plication for diaphragmatic paralysis and eventration: an objective evaluation of short-term and midterm results. J Thorac Cardiovasc Surg 2010;139(6):1452–1456.
45. Higgs SM, Hussain A, Jackson M, Donnelly RJ, Berrisford RG. Long term results of diaphragmatic plication for unilateral diaphragm paralysis. Eur J Cardiothorac Surg 2002;21(2):294–297.
46. Versteegh MI, Braun J, Voigt PG, et al. Diaphragm plication in adult patients with diaphragm paralysis leads to long-term improvement of pulmonary function and level of dyspnea. Eur J Cardiothorac Surg 2007;32(3):449–456.
47. Celik S, Celik M, Aydemir B, Tunckaya C, Okay T, Dogusoy I. Long-term results of diaphragmatic plication in adults with unilateral diaphragm paralysis. J Cardiothorac Surg 2010;5:111.
48. DiMarco AF. Phrenic nerve stimulation in patients with spinal cord injury. Respir Physiol Neurobiol 2009;169(2):200–209.

Imaging of the Diaphragm: Anatomy and Function

Laura K. Nason, MD • Christopher M. Walker, MD • Michael F. McNeeley, MD • Wanaporn Burivong, MD • Corinne L. Fligner, MD • J. David Godwin, MD

RadioGraphics 2012; 32:E51–E70 • **Published online** 10.1148/rg.322115127 • **Content Code:** CH

Page E52 (Figure 3 on page E52. Figure 4 on page E53)
A defect in fusion of the transverse septum to the lateral body wall leads to an anterior (Morgagni) hernia (1) (Figs 3, 4). Morgagni hernias constitute fewer than 10% of congenital diaphragmatic hernias (2).

Page E52 (Figure on page E53)
A posterior (Bochdalek) hernia likely represents a developmental defect of the pleuroperitoneal folds or failure of fusion of the folds and transverse septum with the intercostal muscles (1) (Fig 5). Bochdalek hernias constitute 90% of congenital diaphragmatic hernias and are more common on the left side (1).

Page E57
Dysfunction can be classified as paralysis, weakness, or eventration.

Page E60
Eventration is a congenital thinning of the diaphragmatic muscle that causes a focal bulge.

Page E69
Paralysis is indicated by absence of orthograde excursion on quiet and deep breathing, with paradoxical motion on sniffing. Weakness is indicated by reduced or delayed orthograde excursion on deep breathing, with or without paradoxical motion on sniffing.